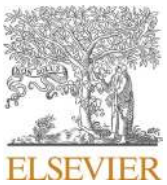
Catena 250 (2025) 108744



Contents lists available at ScienceDirect

Catena

journal homepage: www.elsevier.com/locate/catena



Influence of snow cover and microclimate on soil organic carbon stability in European mountain grasslands

Nicolas Bonfanti [a,b,*], Jérôme Poulenard [b], Jean-Christophe Clément [a], Pierre Barré [d], François Baudin [e], Pavel Dan Turtureanu [f], Mihai Pușcaș [f,g], Amélie Saillard [c], Pablo Raguet [h], Bogdan-Iuliu Hurdu [i], Philippe Choler [c]

[a] Univ. Savoie Mont Blanc, INRAE, CARRTEL, Thonon-Les-Bains, France
[b] Univ. Savoie Mont Blanc, CNRS, EDYTEM, Chambéry, France
[c] Univ. Grenoble Alpes, Univ. Savoie Mont Blanc, CNRS, LECA, Grenoble, France
[d] Laboratoire de Géologie, École Normale Supérieure, CNRS, PSL University, IPSL, Paris, France
[e] Sorbonne Université, CNRS, ISTeP, 75005 Paris, France
[f] A. Borza Botanic Garden, Babeș-Bolyai University, Cluj-Napoca, Romania
[g] Department of Taxonomy and Ecology, Faculty of Biology and Geology, Babeș-Bolyai University, Cluj-Napoca, Romania
[h] Univ. of York, Environment and Geography department, York, United Kingdom
[i] Institute of Biological Research, National Institute of Research and Development for Biological Sciences, Cluj-Napoca, Romania

ARTICLE INFO

Keywords:
Thermal regime
Snow cover duration
Elevation gradient
Freeze
Labile carbon
Rock-Eval® thermal analysis

ABSTRACT

Soil organic carbon (SOC) is crucial for ecosystem function and carbon storage, especially in mountain regions where cooler temperatures limit microbial activity, leading to higher SOC stocks compared to lowlands. However, the available data are insufficient to fully understand the distribution of SOC properties along elevation and snow cover duration gradients. Given that climate change models predict a reduction in snow cover duration, it is essential to better characterize these properties at a finer, mesotopographic scale (e.g., ridges and slopes), corresponding to the distribution of mountain plant communities. This study investigates the impact of microclimate on SOC content and stability in European mountain grasslands. We focused on two types of grasslands on acidic soils to maintain homogeneity in key parameters such as soil properties and plant communities. These grasslands, located across temperate European mountain ranges (Alps, Pyrenees, Vosges, Balkans, Carpathians, Black Forest, Bohemian Forest, and Sudetes), span a gradient of snow cover duration, ranging from frost-exposed ridges dominated by *Carex curvula*, to intermediate grasslands, without frost, dominated by *Nardus stricta*. SOC content and stability were assessed using Rock-Eval® thermal analysis across all sites. The results indicate that microclimate significantly influences SOC properties. Cooler temperatures, driven by elevation and reduced snow cover duration, were associated with increased SOC content but decreased stability. On windy ridges, extended growing seasons combined with intense winter freezing led to higher SOC lability, as freezing slows down mineralization processes. In contrast, intermediate grasslands, with longer growing seasons, showed enhanced SOC stability due to higher decomposition activity. These findings provide valuable insights into how SOC properties may evolve under climate change, particularly in relation to rising temperatures and shifting snow cover dynamics.

1. Introduction

Cold ecosystems, such as those at high latitudes and elevations, contain higher stocks of soil organic carbon (SOC) compared to warmer ecosystems (Budge et al., 2011; Davidson and Janssens, 2006; RMQS, 2017). These ecosystems also hold a significant portion of easily decomposable SOC, with an elevation-driven increase in labile carbon pools within surface horizons (Djukic et al., 2010; Leifeld et al., 2009). The mean residence time of SOC is extended in these environments due to the stabilizing effects of low temperatures, particularly during winter when snow covers the soil and reduces microbial mineralization rates (Budge et al., 2011; Ibanez et al., 2021; Leifeld et al., 2009; Saccone

* Corresponding author.
E-mail address: nicolas.bonfanti.usmb@gmail.com (N. Bonfanti).

https://doi.org/10.1016/j.catena.2025.108744
Received 9 October 2024; Received in revised form 17 January 2025; Accepted 19 January 2025
Available online 5 February 2025
0341-8162/© 2025 The Author(s). Published by Elsevier B.V. This is an open access article under the CC BY license (http://creativecommons.org/licenses/by/4.0/).

et al., 2013). As a result, these SOC stocks are considered highly vulnerable to climate warming (Khedim et al., 2023). Rising temperatures initiate positive feedback by accelerating the mineralization of labile SOC pools that were previously stabilized by cold conditions, leading to increased greenhouse gas (GHG) emissions that further intensify climate change (Davidson and Janssens, 2006). This positive feedback is well-documented in high-latitude environments, particularly in permafrost regions (Hilton et al., 2015), and plays a crucial role in predicting and modeling the carbon cycle's response to climate change (Voigt et al., 2017), and in anticipating shifts in ecosystem functioning. Similar feedback mechanisms are expected in high-elevation European zones, where, since the 1980 s, the warming rate has been about twice the global average (EEA, 2024). Understanding the spatial distribution of SOC, particularly the influence of climate parameters like thermal regime on its distribution, is essential for predicting its response to warming in these cold ecosystems. Furthermore, European mountain regions, as climate change hotspots, offer a unique context for examining SOC properties (stocks and stability) across gradients of snow cover duration.

SOC stability is typically assessed by distinguishing different pools based on their stability, ranging from labile to stable pools, according to the chemical nature of SOC and its mineral interactions (Bernoux et al., 1998; Lavallee et al., 2020; Von Lützow et al., 2007). SOC biogeochemical stability determines the balance between the labile pool, which is easily mineralizable, and the stable pool, which is recalcitrant. The larger the labile pool relative to the stable pool, the less stable the overall SOC stock. Various methodologies exist for fractionating SOC pools, including size and density fractionation, where fraction size serves as a proxy for stable pools (mineral-associated organic matter, MAOM) and labile pools (particulate organic matter, POM) (Balesdent et al., 1998; Buyanovsky et al., 1994; Lavallee et al., 2020; Michalet et al., 2002). A growing approach involves using SOC's thermal stability as a proxy for its environmental persistence. Recent studies employing Rock-Eval® analysis have demonstrated that indicators derived from thermograms, reflecting SOM thermal stability or chemical composition, can be linked to SOM biogeochemical stability (Barré et al., 2016; Cécillon et al., 2018). Comparisons between thermal analysis and other methods of assessing SOM stability, such as physical fractionation (Cécillon et al., 2021, 2018; Gregorich et al., 2015; Saenger et al., 2015) or incubation experiments (Plante et al., 2011), have shown strong correlations. The RockEval technique stands out for its ability to rapidly estimate SOC stability with minimal equipment requirements and low costs, enabling the analysis of a large number of samples efficiently.

Despite the limited use of thermal techniques in characterizing mountain SOC, recent findings indicate substantial SOC lability in these areas (Delahaie et al., 2023), likely due to the higher preservation of mineralizable SOC due to low temperatures limiting SOC mineralization in mountains. However, other factors than temperatures influencing SOC stability must also be considered, including SOC chemistry (Amelung et al., 2008; Lorenz et al., 2007), parent material characteristics (Doetterl et al., 2015; Heckman et al., 2009), soil age (Khedim et al., 2021), soil pH (Andersson and Nilsson, 2001), soil structure (Virto et al., 2010), particle size distribution (Derrien et al., 2016), content of oxyhydroxides and ions (Moni et al., 2010), microbial activity (Schimel and Schaeffer, 2012; Schinner, 1982), land use (Guidi et al., 2014; Hafner et al., 2012; Li et al., 2015), land cover and plant traits (such as productivity and resource strategy) (Dorji et al., 2020; Li et al., 2015), litter quality (Bernard et al., 2019; Garcia-Pausas et al., 2012; Silver and Miya, 2001), and soil (micro)climate (Li et al., 2018). These parameters naturally co-vary and are interconnected, making it challenging to isolate and quantify their individual contributions to SOC stability.

There is increasing recognition that microclimate plays a pivotal role in shaping species distribution and ecosystem properties (De Frenne et al., 2013; Kemppinen et al., 2024). In mountainous regions, soil microclimate varies significantly both on a large scale (elevation gradient) and on a smaller scale due to topographic and snow cover variations. The thermal regime, including energy received by the soil (growing degree days, GDD) and frost intensity (freezing degree days, FDD) (Choler, 2015, 2005), strongly influences the activity of organisms involved in carbon inputs and outputs. Soil climate modulates species distribution and ecosystem properties such as organic matter inputs, mineralization activity and thus SOC properties. Also, topographical variations control the height and duration of the winter snowpack, impacting seasonal variations in soil temperature and moisture (Zhang, 2005). In sites where snow melts late, soils remain near 0 °C throughout winter under the snowpack, allowing for slow mineralization activity (Clément et al., 2012). Conversely, in areas with early snowmelt, soils may have a longer growing season but also experience periods of soil freezing that disrupt biological activity (Baptist et al., 2010; Buckeridge and Grogan, 2010; Jusselme et al., 2016; Michalet et al., 2002; Saccone et al., 2013).

We focused on two distinct plant communities that are widely distributed in European temperate mountains: *Carex curvula*-dominated alpine grasslands (CCU), characterized by winter soil freezing and an extended growing season, and *Nardus stricta*-dominated subalpine-alpine grasslands (NST), which, at a given elevation, have a shorter growing season but without winter soil freezing. Our objective was to explore the influence of (micro)climatic parameters on SOC properties, estimated by the Rock-Eval® method, across mountain grasslands. This analysis was conducted on a broad biogeographical scale, covering temperate European mountain ranges including the Alps, Pyrenees, Vosges, Balkans, Carpathians, Black Forest, Bohemian Forest, and Sudetes. By concentrating on similar habitats, we ensured consistent local conditions despite the geographical distances between sampling sites. Both grassland communities grow on acidic soils and share similar soil properties (see Fig. S3; Geremia et al., (2016); Puşcaş and Choler, (2012).

We explored the role of microclimate on SOC properties, specifically growing season length (GSL, GDD), freezing season length (FSL, FDD), and regional water regime (water balance, rainfall). We hypothesized that SOC properties were influenced by the soil temperature regime and thus structured along the growing season (H1) and along a gradient of freezing (H2), both gradients are influenced by the snow cover duration. Additionally, given that water regimes influence the activity of both producers and decomposers, we hypothesized that SOC properties are influenced by regional climatic factors, particularly precipitation (H3), and by vegetation characteristics (H4), as they control the quantity and quality of litter inputs.

2. Materials & methods

2.1. Study sites – Sampling protocol

Our study focused on two types of mountain grasslands that developed on acidic soils, with a pH gradient ranging from 3.5 to 4.5 between sites. *Carex curvula*-dominated grasslands (CCU) represent late-successional alpine communities, typically found on siliceous bedrock, and are characterized by winter soil freezing (Geremia et al., 2016; Puşcaş and Choler, 2012; Schlag and Erschbamer, 2000). In contrast, *Nardus stricta*-dominated grasslands (NST) are subalpine-alpine grasslands primarily located in concave topography, where winter snow cover insulates the soil from freezing (Gennai et al., 2014). These grasslands span a gradient of snow cover duration (Fig. 1). In both plant communities, the dominant species comprise the majority of the phytomass, suggesting that these species exert a significant influence on ecosystem structure and functioning (Grime, 1998; Whitham et al., 2006).

The study area encompasses all the European temperate mountain ranges of the so-called European Alpine System (Ozenda, 1985) and includes the Pyrenees, Alps, Black Forest, Bohemian Forest, Sudetes, Carpathians, Vosges, and Balkans. Field sampling was conducted as part of a long-term monitoring program within the ODYSSEE project (https

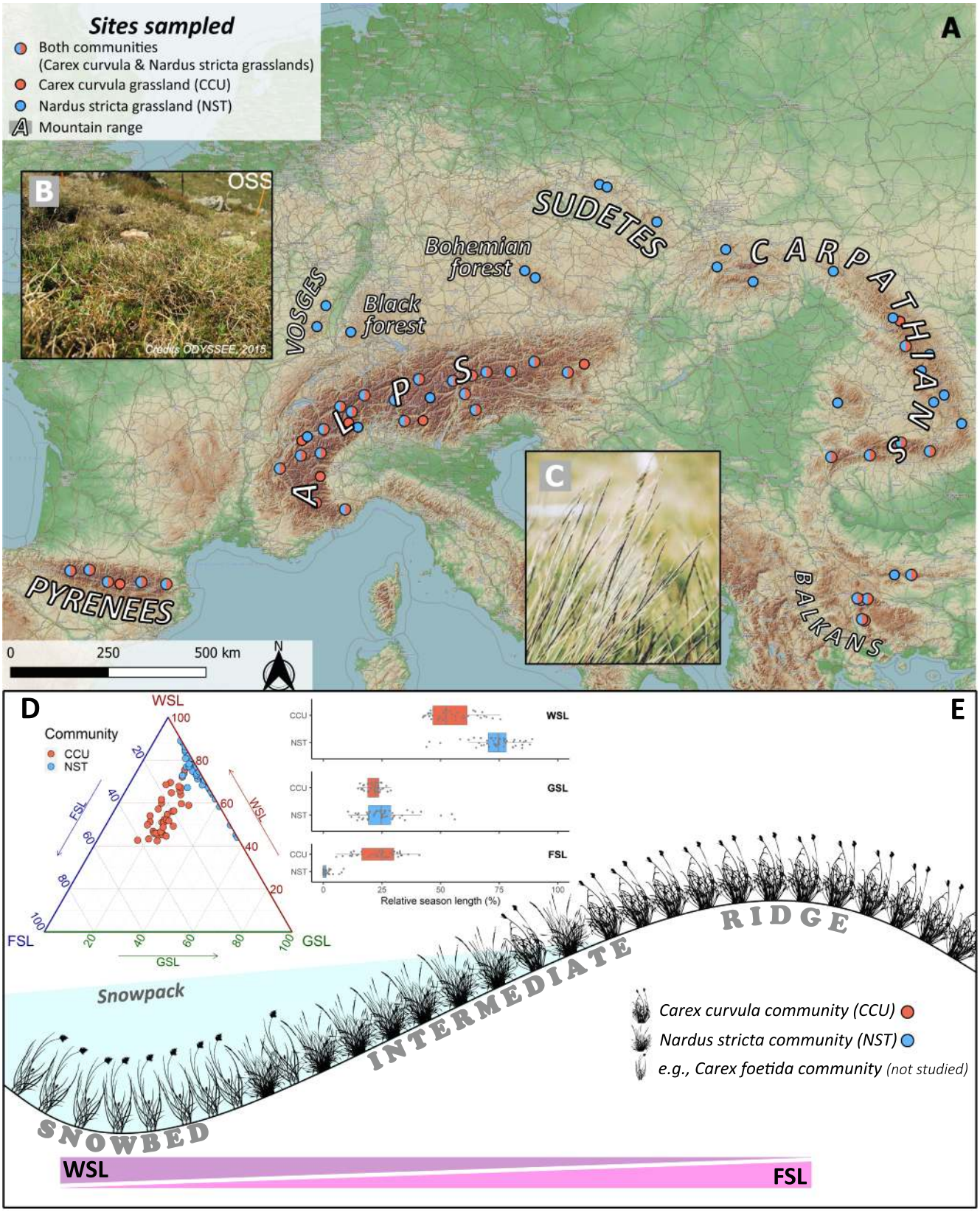


Fig. 1. Sampling design. Map of sampling sites (A); *Carex curvula* grassland (CCU) (B); *Nardus stricta* grassland (NST) (C); Thermal regime of both communities average over: Freezing Season Length (FSL, i.e., annual number of days with mean daily temperature < -1°C), Growing Season Length (GSL, annual number of days between NDVI onset and offset) and Winter Season Length (WSL, i.e., annual number of days with mean temperature > -1°C out of the growing season), (D); Schematic and theoretical representation of mesotopographic/snow cover duration gradient that can be found in the Alps (E; see also Fig. S1 for temperature series of both communities). Note that the sampling was not done along this gradient but within both communities throughout the mountain range.

://odyssee.granturi.ubbcluj.ro/project-description/). We employed a paired sampling scheme based on an 80 km × 80 km grid defined by the European Terrestrial Reference System (ETRS 89). Wherever possible, both grassland types (CCU and NST) were sampled within the same grid cell. Sampling took place within a 10 m × 10 m quadrat dominated by one of the target species (CCU or NST), with > 25 % cover for the dominant species (Turtureanu et al., 2023, 2020). A total of 100 sites were surveyed (Fig. 1): 36 grid cells contained both plant communities, 22 grid cells had only NST, and 6 grid cells had only CCU. Some grids contained only one of the two communities because the elevation was too low for CCU grasslands.

At each site (100 m^2), five soil samples (0–10 cm depth) were collected from the four corners and the center of the quadrat, and then combined to create a composite soil sample.

2.2. Soil analysis

After drying and grinding the composite soil samples, SOC and total nitrogen contents were measured using a CHN elemental analyzer (Flash EA 1112, Thermo Electron Corporation, Thermo Fisher). Soil pH was measured using a pH meter (inoLab 7110, WTW, Germany) following the international standard ISO 10390–2005.

2.2.1. SOC stability

SOC stability was assessed using a Rock-Eval 6® analyzer (RE6) (Vinci Technologies, France), following a protocol adapted for soil analysis (Barré et al., 2023; see also Fig. S14). The RockEval method is based on the principle that the thermal stability of organic matter serves as a proxy for its biogeochemical stability. For each sample approximately 60 mg of dried soil were subjected to pyrolyze in an inert N_2 atmosphere, with temperatures increasing from 200 °C to 650 °C at a rate of 30 °C/min (pyrolyze phase). The remaining soil was then oxidized in an oxygenated environment, with temperatures ranging from 300 °C to 850 °C at a rate of 20 °C/min (oxidation phase). Hydrocarbon compounds (HC) released during the pyrolysis phase were continuously monitored using a Flame Ionization Detector (FID), whereas CO_2, and CO released during both phases (pyrolysis and oxidation) were monitored using an Infrared Cell (IR). The total organic carbon can be calculated as the sum of carbon fractions (HC + CO + CO_2) over the two phases, showing good correlation with C content from CHN elemental analyzer (Fig. S4.A).

Several indices derived from the ratios of carbon forms (CO_2, CO, HC) released during different phases (pyrolysis and oxidation) of Rock-Eval® analysis have been proposed as indicators of SOC stability (Barré et al., 2016; Disnar et al., 2003; Sebag et al., 2016). Due to the high quantity of parameters proposed, we selected only six complementary parameters in our study (Fig. S14). We used Hydrogen Index (HI), Oxygen Index (OI), PC/TOC ratio, T50CO2pyr, i_index, and R_index (Equations (1) and (2), Fig. S14). HI and OI are considered proxies for SOM stoichiometry, reflecting the H:C and O:C ratios, respectively. Hydrogen-rich SOM (high HI index) are generally considered as more labile than oxygen-rich SOM, as aliphatic chain required less activation energy to be decomposed than more complex functional groups (aromatic, carbonyl, carboxyl, etc…) (Laub et al., 2020). T50CO2pyr, defined as the temperature (°C) at which 50 % of the CO_2 is released during the pyrolysis phase, was employed as an additional parameter for evaluating SOC thermal stability, following Soucémarianadin et al., (2018). This parameter has been validated on bare fallow experiments as a reliable indicator of SOC biogeochemical stability (Barré et al., 2016; Cécillon et al., 2018, 2021). The more thermal energy is necessary to release 50 % of CO_2, the more thermally and biogeochemically stable the SOM. I_index and R_index represent the degree of immaturity and refractory of SOM respectively (Equations (2), Fig. S14). These indices are proposed by Sebag et al. (2016) to estimate SOM biogeochemical stability with i_index anticorrelated with SOM stability and R_index positively correlated.

$$HI = \frac{HC}{TOC} \times 100;\ OI = \frac{CO_2 + CO}{TOC} \times 100;\ PC_TOC = \frac{CO_{2_{pyr}} + CO_{pyr} + HC_{pyr}}{TOC} \quad (1)$$

With: HC = hydrocarbon quantity measured with FID; CO_2 and CO = quantity of CO_2 and CO measured with FTIR. X_{pyr} = quantity of x element measured during pyrolysis phase.

$$i_index = \log\left(\frac{A1 + A2}{A3}\right); R_index = \frac{A3 + A4}{100} \quad (2)$$

With: A1, A2, A3, A4 for area of pyrogram of labile polymers (200–340 °C), resistant biopolymers (340–400 °C), immature geopolymers (400–460 °C) and refractory geopolymers more than 460 °C) respectively (Sebag et al., 2016).

2.3. Climatic variables

2.3.1. Regional-scale climate

To characterize the regional thermal and hydrological regimes at each site, we utilized gridded climate variables from WorldClim at a 30-second resolution (Fick and Hijmans, 2017). Climate normals for the period 1960–1990 were adjusted for distance and elevation differences between the center of each grid cell and the specific plot location. We extracted data on the average temperature of the growing season (**T_AVG**, °C), and the daily minimum temperature during the growing season (**T_MIN**, °C). These metrics were selected because average temperature is widely used as a general indicator, while minimum temperature provides insight into frost intensity. Estimates of average shortwave radiation entering the atmosphere for the period 1985–2005 (**SRAD**, J/cm^2) were obtained from the Helioclim satellite, which has a resolution of 20 km (SoDa, 2015). Additionally, monthly surface water balance and soil water extractability data, with a resolution of 1/24 degree, were sourced from Terraclim averages spanning 1981–2010 (Abatzoglou et al., 2018; Stephenson, 1998). This dataset included precipitation (**PREC**, mm), actual evapotranspiration (**AET**, mm), and water deficit (**DEF** = PREC − AET, mm).

2.3.2. In-situ temperature measurements

Soil temperature was monitored using miniaturized, standalone data loggers (HOBO pendant 64 K, Onset Company) at each plot from 2014 to 2019, with monitoring duration ranging from 2 to 5 years depending on the site. This monitoring enabled the calculation of Growing Degree Days (**GDD**, °C) and Freezing Degree Days (**FDD**, °C). GDD represents the sum of daily average temperatures above 1 °C from January 1 to July 31, while FDD represents the sum of daily average temperatures below −1°C over the same period. Additionally, the number of freezing days per year, which indicates the duration of the freezing season (Freezing Season Length, **FSL**, days), was determined by counting the days when the daily average soil temperature dropped below −1°C throughout the year.

2.4. Ecosystem phenology

The ecosystem phenology was estimated using the remotely-sensed Normalized Difference Vegetation Index (NDVI) obtained from the MOD09Q1 Terra Collection 6 products, which consist of 250 m resolution 8 days composites of the Moderate Resolution Spectroradiometer (MODIS) sensor on board the Terra satellite. Data processing is described extensively in Choler (2023). These data, averaged over the 2000–2018 period, were used to determine the dates of vegetation onset (**ONSET**; Julian day) and offset (**OFFSET**; Julian day). Additionally, this analysis allowed the computation of growing season length (**GSL**, day, Choler (2015). We employed remote sensing to calculate GSL due to the ability to average over a longer period, compensating for the lack of in-situ measurements.

In contrast, we used in-situ measurements for FSL because remote sensing could not provide soil temperature and detect soil freezing. By combining GSL and FSL measurements, we calculated the Winter Season Length (**WSL**) using Equation (3), which represents how long the soil remained snow-covered or unfrozen outside the growing season. While the absolute values may not be exact, they were comparable across sites. For instance, a day without snow cover during winter where the average soil temperature exceeds −1°C was included in the WSL, even if snow was not present; the soil conditions on such a day are consistent with those of a WSL day. To verify these results, we also calculated GSL by counting the number of days when the average soil temperature was above 1 °C. Both methods for calculating GSL (NDVI and temperature > 1°C) showed correlated results, although the NDVI method tended to underestimate GSL (see Fig. S2).

$$GSL + FSL + WSL = 365 \quad (3)$$

With: Growing Season Length GSL = number of days between $ONSET_{NDVI}$ and $OFFSET_{NDVI}$;

Freezing Season Length FSL = number of days in a year during which the average daily temperature < -1°C; Winter Season Length WSL = number of days in a year out of GS and without soil freezing (i.e., snow-cover or senescence).

2.5. Plant communities

The floristic composition of the plots was surveyed using semi-quantitative estimates of plant cover (Braun-Blanquet, 1964), using a 6-levels scale (+ = less than 5 %; 1 = 5–10 %; 2 = 10–25 %; 3 = 25–50 %; 4 = 50—75 %; 5 = more than 75 %). On each plot, specific leaf area (**SLA**, cm^2/g), plant height (**Hveg**, cm), aboveground biomass (**AGB**, g/m^2), and its stoichiometric composition (carbon and nitrogen content, **C:N**) were measured on the dominant species (CCU or NST) following the methods outlined in Garnier et al. (2001) and Turtureanu et al., (2020). Annual plant productivity was evaluated by integrating NDVI (see above) over the duration of the growing season and averaged over the 2000–2018 period (Choler et al., 2021).

2.6. Statistical analysis

2.6.1. Generalized linear model and model selection

To determine the main explanatory variables influencing SOC content, we conducted generalized linear model selection by using the "glmulti" package (Calcagno et al., 2020). The statistical significance of each variable was assessed based on their prevalence in model selection via AIC criteria and their contribution to the overall model. Linear relationships were established using the lme4 package (Bates et al., 2015). Normality and homoscedasticity of the residuals were systematically evaluated for all interpreted models. To estimate the weight of each variable on explanation of SOC content variance, we used partial R^2, i.e., the variance explained by each variable given others are included, by using "r2glmm" package (Jaeger, 2017).

2.6.2. Multivariate analysis – Biogeochemical stability index calculation

To reduce the dimensionality of the explanatory dataset, we conducted a principal component analysis (PCA) on each of the following groups of variables: climate, vegetation, and SOC properties (Fig. S4). Climate integrated thermal parameters (SRAD, GDD, TAVG, TMIN, FDD), season lengths (GSL, FSL) and hydric parameters (PREC and DEF) (Fig. S4.C). Vegetation PCA included SLA, C:N ratio of aboveground biomass, aboveground biomass, vegetation height and NDVI (Fig. S4.D). SOC properties PCA integrated T50CO2pyr, OI, HI, i_index, R_index and PC_TOC (see § for signification of each index) (Fig. S4.B). The aim of SOC PCA was to obtain a single, standardized SOC biogeochemical stability estimator that maximized the inter-sample variance of the Rock-Eval indices (representing SOM chemistry and thermal stability). For this, we used the coordinates on axis 1 of the PCA of SOC stability indices (Fig. S4.B). The values on this axis (hereafter called **C_stab**) allowed to qualitatively discuss variations in biogeochemical stability rather than focusing on compartmental values of active and stable C. The PCA of the Rock-Eval indices revealed a stability gradient along axis 1 (Fig. S4.B), which was integrated into a structural equation modeling approach (SEM, see next section) hereafter called "**C_stab**": high C_stab value corresponded to more stable SOC. Similarly, axis 1 of the plant-trait PCA was used to condense plant characteristics into a gradient of productivity (Fig. S4.D), which was then incorporated into the SEM (**VG**): high VG values corresponded to high productivity.

Multivariate analysis with two tables were conducted to illustrate co-structures and patterns between climatic variables and SOC properties, as well as between climatic data and plant traits, and between plant traits and SOC properties. To identify the climatic variables that best explain SOC properties, and the SOC properties which were best explained by climate, co-inertia analyzes were used. These analyzes aimed to reveal covariations and help select the most relevant variables for the SEM, focusing on variables carrying the most inertia between climate and SOC stability. Co-inertia analysis was evaluated using a Monte Carlo approach and permutation tests. The co-inertia analysis was performed with the "ade4" package (Dray et al., 2023) and PCA using the "factomineR" package (Lê et al., 2008). Due to elevational differences between communities, we also conducted separate analysis for each of them (Fig. 4 and see Figs. S5 – S8).

2.6.3. Structural equation modeling (SEM)

We implemented SEM to compare different causal relationships among variables and determined the direct and indirect effect of each variable. For reminder, an indirect effect of X1 on Y means that the effect of X1 is mediated by another variable X2 (for example X1 → X2 → Y) (Grace, 2006).

Step1: Structure set up; The structure was developed based on the scientific literature reviewed in the introduction, which highlights that climatic factors (temperature, humidity, and phenology) and plant traits influence SOC characteristics, including stability and content. Given that climate also affects functional plant traits such as productivity, vegetation was positioned as an intermediary factor in the framework. It was assumed that the relationships among these factors were linear. The framework posited that climate and pH exerted an exogenous influence on both vegetation and SOC properties. Subsequently, it was proposed that vegetation regulate SOC properties, aligning with previous research demonstrating that vegetation type and productivity affect SOC stability and content (e.g., Budge et al., (2011); Djukic et al., (2010). Separate models were developed for *Nardus stricta*-dominated (NST) and *Carex curvula*-dominated (CCU) grasslands to compare effect size in two different thermal regimes.

Step2: Model suitability assessment; The model structure was then validated using our standardized data to account for scale differences among variables. To meet the assumptions of residual normality and homoscedasticity, log or square root transformations were applied as necessary. Linear relationships were fitted using the "lme4" package (Bates et al., 2015), and the model structure was analyzed with the "piecewiseSEM" package (Lefcheck et al., 2023), employing maximum likelihood for estimation. The overall model fit was evaluated through several methods: a separator test (to check if significant correlations were integrated into the model), the Chi-squared test (to assess the model's suitability), and the Root Mean Square Error of Approximation (RMSEA). An RMSEA value below 0.05 was considered indicative of a "close fit" between the model and the data, while a value below 0.08 was deemed acceptable for a reasonable model-data fit (Browne and Cudeck, 1992; Jöreskog and Sörbom, 1993; Xia and Yang, 2019). Finally, an assessment of the model's local areas of weakness was conducted, with a focus on evaluating each relationship individually.

Step3: Model interpretation; The statistical relationships among variables within the model were interpreted based on their direction

(positive or negative) and their magnitude (standardized estimator for the entire model). The effects of each variable were evaluated through bootstrapping with 500 iterations, which allowed for the measurement of the significance of each effect and the assessment of their nature: direct effects, indirect effects (partial correlations), and mediating effects.

3. Results

3.1. Soil microclimate

Both grassland communities exhibited distinct thermal regimes. CCU were characterized by extended winter freezing (high Freezing Season Length – FSL and Freezing Degree Days – FDD). In contrast, NST grasslands did not experience any soil freezing (Fig. 1; see also Fig. S1 for temperature chronologies). As a result, the seasonal distribution between growing season (GSL) and winter season (WSL) was more distinct in NST (GSL ~ WSL, $R^2 = 0.96$). For CCU, the seasonal dynamics were primarily driven by freezing season length (FSL) and winter season length (WSL) (FSL ~ WSL, $R^2 = 0.85$), with growing season length (GSL) showing minimal variation (see Table S2). Moreover, CCU grasslands were located at higher altitudes compared to NST grasslands (Fig. S3). This elevation difference resulted in a narrower range of temperature (growing degree day – GDD, mean daily temperature – T_AVG) and growing season length for CCU grasslands. However, freezing season length and freezing degree day displayed a broader range of variation in CCU grasslands (Fig. 1, Fig. S3).

3.2. SOM property indicators

Rock-Eval analysis demonstrated a strong correlation between total organic carbon measured by Rock-Eval and total organic carbon measured using an elemental analyzer, though some deviation was observed at higher concentrations ($y = 0.85x$, $R^2 = 0.99$, see Fig. S4.A). While total SOC content was weakly correlated with SOC stability indices, the stability indices themselves were strongly correlated to each other (Fig. S4.B). A clear thermal stability gradient emerged along the axis 1 of the PCA which constrain 49.4 % of variance, where PC/TOC and I_index were positively correlated, while T50CO2pyr and R_index were negatively correlated (Fig. S4.B, see also Fig. S13). Therefore, this axis 1 of PCA RockEval indices was inversely related to SOC thermal stability, with lower values representing greater stability. This thermal stability gradient was also associated with a SOC chemistry gradient represented by the hydrogen index, HI, and oxygen index, OI, so that we considered this gradient as biogeochemical stability gradient (C_stab).

Indicators of SOC stability showed globally higher stability for NST grasslands than for CCU grasslands (Fig. S3). For instance, mean R_index was 0.499 (± 0.034) for CCU and 0.516 (± 0.0315) for NST (Pvalue *t* test < 0.05) and mean HI was 373.2 (± 26.6) for CCU and 346.6 (± 50.7) for NST (Pvalue *t* test < 0.05). Finally, SOC content did not differ significantly between both grassland types (Fig. S3).

3.3. Climatic factors contribution

SOC content showed no consistent pattern with elevation (Fig. 2, Table S1). Yet, the biogeochemical stability gradient of SOC was inversely related to elevation, meaning that SOC at higher elevations was less stable, except for CCU where an opposite trend was observed

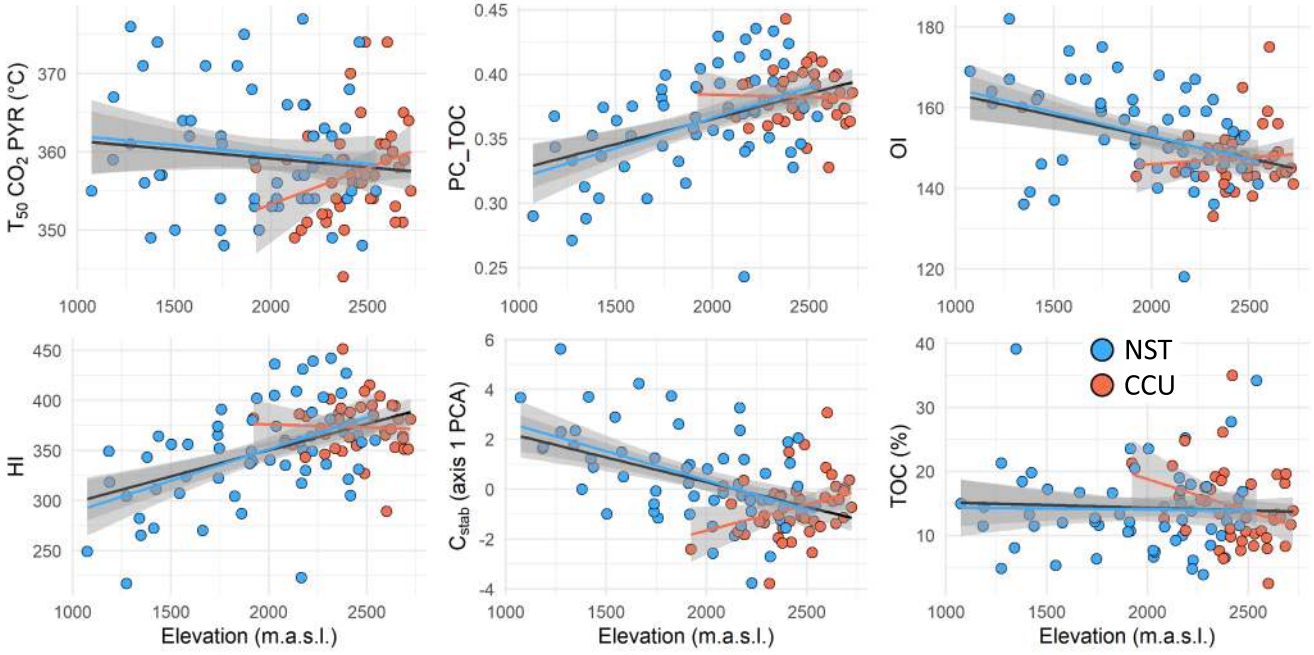


Fig. 2. SOC properties (content and stability) along the elevation gradient. TOC represents total organic carbon content, measured using an elemental analyzer and expressed as a percentage ($g_{TOC}/g_{dry\ soil} \times 100$). SOC stability was evaluated using RockEval® indices, including T50CO2pyr, OI, PC_TOC, and HI. RockEval analysis provides a proxy for the biogeochemical stability of SOC by assessing its thermal stability. During the analysis, soil samples were heated in an oven, and carbon release was quantified by monitoring CO, CO_2, and HC emissions across two phases: pyrolysis (under an N_2 atmosphere) and oxidation (under aerobic conditions). The indices used here are: **T50CO2pyr**, temperature (°C) at which 50 % of the carbon is released as CO_2 during the pyrolysis phase; **OI** (Oxygen Index), the ratio of the sum of CO and CO_2 emissions (from both phases) to TOC. A high OI indicates more recalcitrant organic matter; **HI** (Hydrogen Index), the ratio of HC emissions (from both phases) to TOC. Hydrogen-rich organic matter is generally more labile; **PC_TOC**: the ratio of pyrolysable carbon to TOC, calculated as the sum of CO, CO_2, and HC emissions during the pyrolysis phase relative to TOC. This serves as a proxy for carbon lability. Also, to derive a single composite index of SOC stability that integrates correlations among these indices, we performed a PCA and used the coordinates on the first principal axis: C_stab (multiplied by −1 for consistence, see Fig. S4.B). Linear regressions were conducted between these variables and elevation for CCU (red), NST (blue), and both communities combined (black). See Table S1 for the significance of the linear regressions.

(Fig. 2, Table S1, Figs. S4.B and S13).

The SOC content and SOC biogeochemical stability gradient were primarily influenced by the temperature/elevation gradient, represented by growing degree days (GDD) and growing season length (GSL) (Fig. 3). This temperature-driven gradient accounted for the majority of the variability observed in SOC properties. In the SOC content model, GDD and GSL contributed 19 % and 17.8 % of the explained variance (R^2), respectively (Fig. 3.A, Table S3). GDD decreased the SOC content while GSL increased it. Co-inertia analysis showed that GSL and GDD accounted for 20.9 % and 19.7 % of the total climatic contribution to the association with SOC stability indices, respectively (Fig. 3.B, Table S4). Co-inertia showed also that higher GSL and GDD led to higher SOC biogeochemical stability (Fig. 3.B).

Secondly, a freezing gradient, represented by freezing season length (FSL) and freezing degree days (FDD), emerged as a significant factor. FSL and FDD contributed 10.1 % and 9.4 % of the explained variance in SOC content, respectively (Fig. 3.A, Table S3). Both factors increased the SOC content. These parameters also accounted for 11.6 % and 9.8 % of the co-inertia between climate variables and SOC stability indices, respectively (Fig. 3.B, Table S4). This freezing gradient is mainly driven by snow cover duration and therefore reflected the mesotopographical gradient (Fig. 3.B, Fig. S5.A). Co-inertia showed that higher freezing intensity led to lower SOC biogeochemical stability (Fig. 3.B).

Thirdly, regional water-related variables, including precipitation (PREC) and water deficit (DEF), also played a role in determining SOC content and stability. PREC and DEF explained 7.7 % and 0.1 % of SOC content variance, respectively (Fig. 3.A, Table S3). For SOC stability, DEF and PREC contributed 3.2 % and 1.1 % to coinertia, respectively (Fig. 3.B, Table S4, axis 2). Higher DEF was associated with increase in SOC biogeochemical stability and decrease in SOC content (Fig. S3).

Within CCU, SOC stability was predominantly positively influenced by the water deficit (DEF) (19 % of coinertia contribution, Table S4, Fig. S5.D, Fig. S13), while SOC content was mainly determined by temperature-related factors (GDD = 17.8 % and GSL = 18.1 % of the explained variance, Table S3, Fig. 4.B). In contrast, within NST, the GDD/GSL gradient primarily explained SOC stability (GDD = 19.5 % and GSL = 22.7 % of coinertia contribution, Table S4, Fig. S5.C), whereas the regional water regime (PREC), played the most significant role in determining negatively SOC content (25.0 % of the explained variance, Table S3, Fig. S5.A, Fig. S13).

A linear model including both elevation and freezing season length (FSL), which represents the snow cover gradient, revealed a negative relationship between SOC stability and both elevation and FSL (R^2 = 0.42, Table 1). These relationships were thoroughly tested and validated within the SEM (Fig. 4), providing a robust approach to isolate and analyze the individual effects of each parameter.

3.4. Soil pH contribution

A particularly significant finding was the consistent relationship of soil pH with both SOC stability (Fig. S13) and SOC content (32.3 %, 30.7 % and 48.8 % of the explained variance for both grasslands, NST and CCU respectively, Table S3, Fig. 4, Fig. S13). Despite exhibiting low variation, soil pH was positively correlated with SOC stability and negatively correlated with SOC content.

3.5. Contribution of vegetation

In both communities, a significant correlation was observed between NDVI (a proxy for positive carbon flux into the ecosystem), above-ground biomass (AGB) (representing the living above-ground carbon stock), and the C:N ratio (Figs. S4.D, FS6, FS7). NST grasslands exhibited higher vegetation height (Hveg), AGB, and NDVI compared to CCU, while CCU grasslands showed a higher SLA (Fig. S3).

A gradient of productivity was identified both between and within these two grassland communities (axis 1 of the functional traits PCA, Fig. S4.D; axis 1 of the co-inertia between functional traits and SOC properties, Fig. S7). This productivity gradient was correlated with SOC stability (Fig. S7).

Within the communities, the relationships between vegetation and SOC stability exhibited contrasting patterns (Fig. 4, Figs. S6 and S13). In CCU grasslands, FSL increased productivity, and both factors increased SOC content, while they decreased SOC stability. In NST, GSL had a positive impact on productivity, but the effect of the water regime (precipitation and water deficit) on SOC characteristics was comparatively less significant (Fig. S8). Both SOC stability and SOC content increased with productivity in NST (Fig. 4, Figs. S6 and S13).

4. Discussion

Our results showed that SOC properties in acidic mountain grasslands are consistently varying along mesotopographical gradients. First, the soil thermal regime, governed by snow cover—which is influenced by elevation and mesotopographic position—plays a critical role in controlling soil freezing. In intermediate grasslands (NST), elevation drives changes in SOC, with higher elevations leading to increased SOC content but reduced stability. In contrast, on windy ridges (CCU), freezing season length (FSL) is the main factor, similarly increasing SOC content while reducing stability. Second, other environmental gradients, including water regime and soil pH, significantly impact SOC properties. More acidic soils tend to accumulate higher SOC content, but with lower stability. Thirdly, the characteristics of the plant cover likely drove SOC properties particularly (Fig. 4) through the quality of litter inputs (chemical composition, H:C, C:N, etc…) which is partly controlled by plant traits and functional properties of canopies (SLA, productivity).

4.1. SOC properties in mountain grasslands

The analysis along the elevation gradient requires caution, particularly due to the latitudinal differences between the study sites. However, this approach holds illustrative value, allowing for meaningful comparisons with data from lower altitudes that are similarly distributed across a broad latitudinal range. We showed that SOC biogeochemical stability decreased with elevation (Fig. 2; Table 1), in line with previous research showing that SOC in mountain grasslands tends to be less stable compared to lowland ecosystems. For instance, Delahaie et al. (2023) reported mean T50CO2pyr values between 380 °C and 390 °C in lowland meadows in mainland France, while we observed a lower mean value of 358 °C in our study. Similarly, their average HI value was 210 mg_{HC}/g_{TOC}, whereas we measured an average of 358 mg_{HC}/g_{TOC}. These findings support the hypothesis that SOC in mountain grasslands is highly biogeochemically labile, as suggested by other methods such as mean residence time and physical fractionation (Budge et al., 2011; Leifeld et al., 2009; Saenger et al., 2015). Our results showed that HI negatively correlated with thermal stability, indicating that 'chemically labile' SOC (i.e., which requires less activation energy) dominates in mountain soils. This suggests that SOC stability is primarily the result of environmental stabilization, i.e., that low temperatures limits mineralization activity, leading to the accumulation of labile SOC (Schmidt et al., 2011). Similar to permafrost soils, where climate stabilization effectively sequesters SOC, mountain soils could store SOC that may be easily mineralized under higher temperatures (Jin and Ma, 2021; Schuur et al., 2008; Siewert et al., 2015). This is further supported by Delahaie et al. (2023). This study found a positive correlation between T50CO2pyr and MAT ($r = 0.24$, $p < 0.001$), and a negative correlation between HI and MAT ($r = -0.20$, $p < 0.001$).

4.2. Freezing season length and SOC properties

SOC properties seem to be influenced by frost intensity (freezing season length and freezing degree day), which is closely linked to the snow cover regime during winter. In areas where snow does not

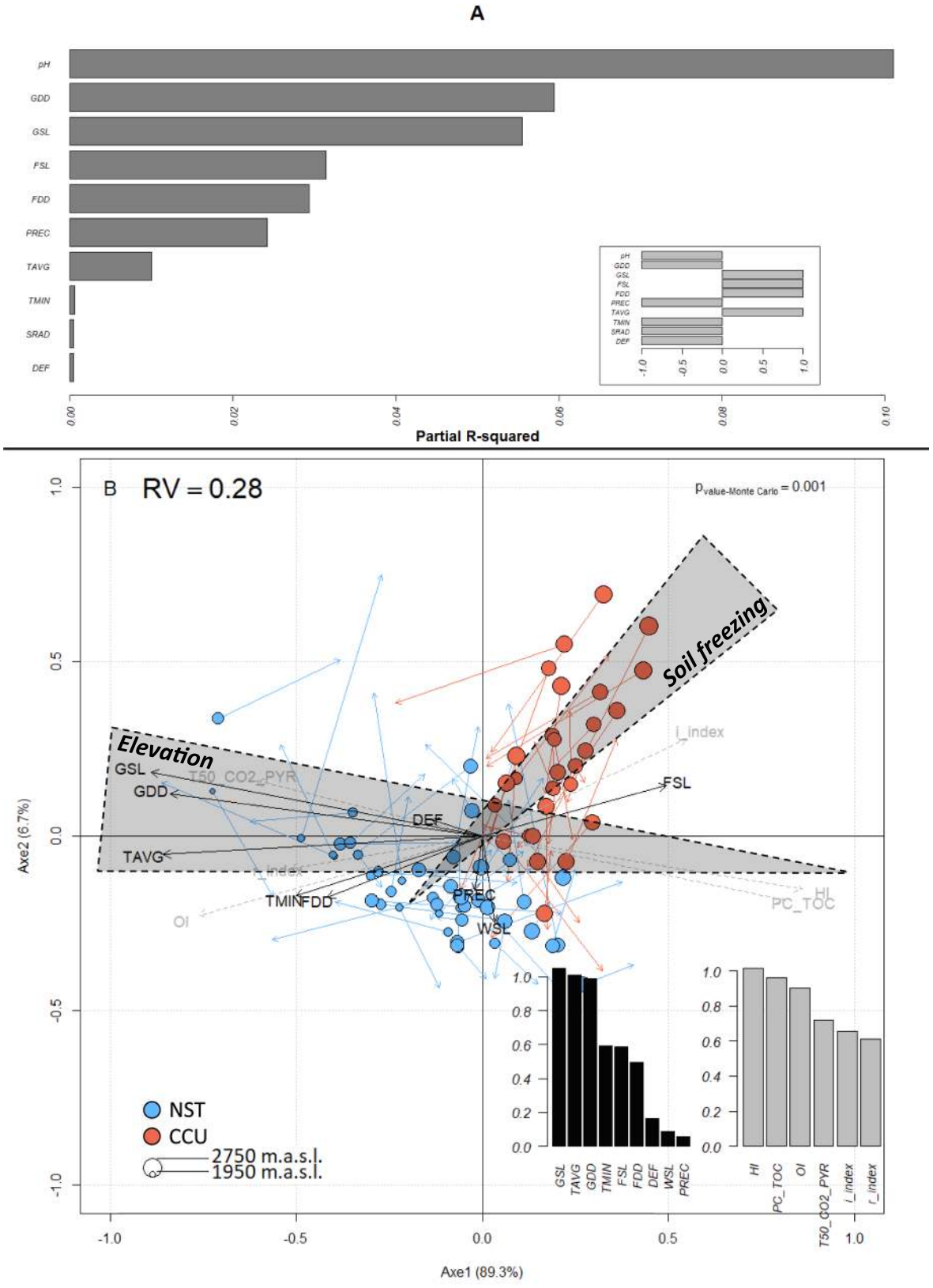


Fig. 3. Climate-SOC properties relationships. (**A**) Model-averaged importance of variables in explaining total SOC content. The value represents the relative importance of each variable in explaining the variance in SOC content: higher values indicate a greater proportion of variance explained. Variables include: pH (soil pH), GDD (growing degree days), GSL (growing season length), FSL (freezing season length), PREC (precipitation), TAVG (daily average temperature), Tmin (mean minimum daily temperature), SRAD (solar radiation), and DEF (water deficit, calculated as precipitation minus actual evapotranspiration). (**B**) Co-inertia analysis between climatic parameters and SOC stability indices (refer to Fig. 2 caption for index definitions) for both CCU and NST. Point size corresponds to site elevation. See Fig. S5 for separate results within each community.

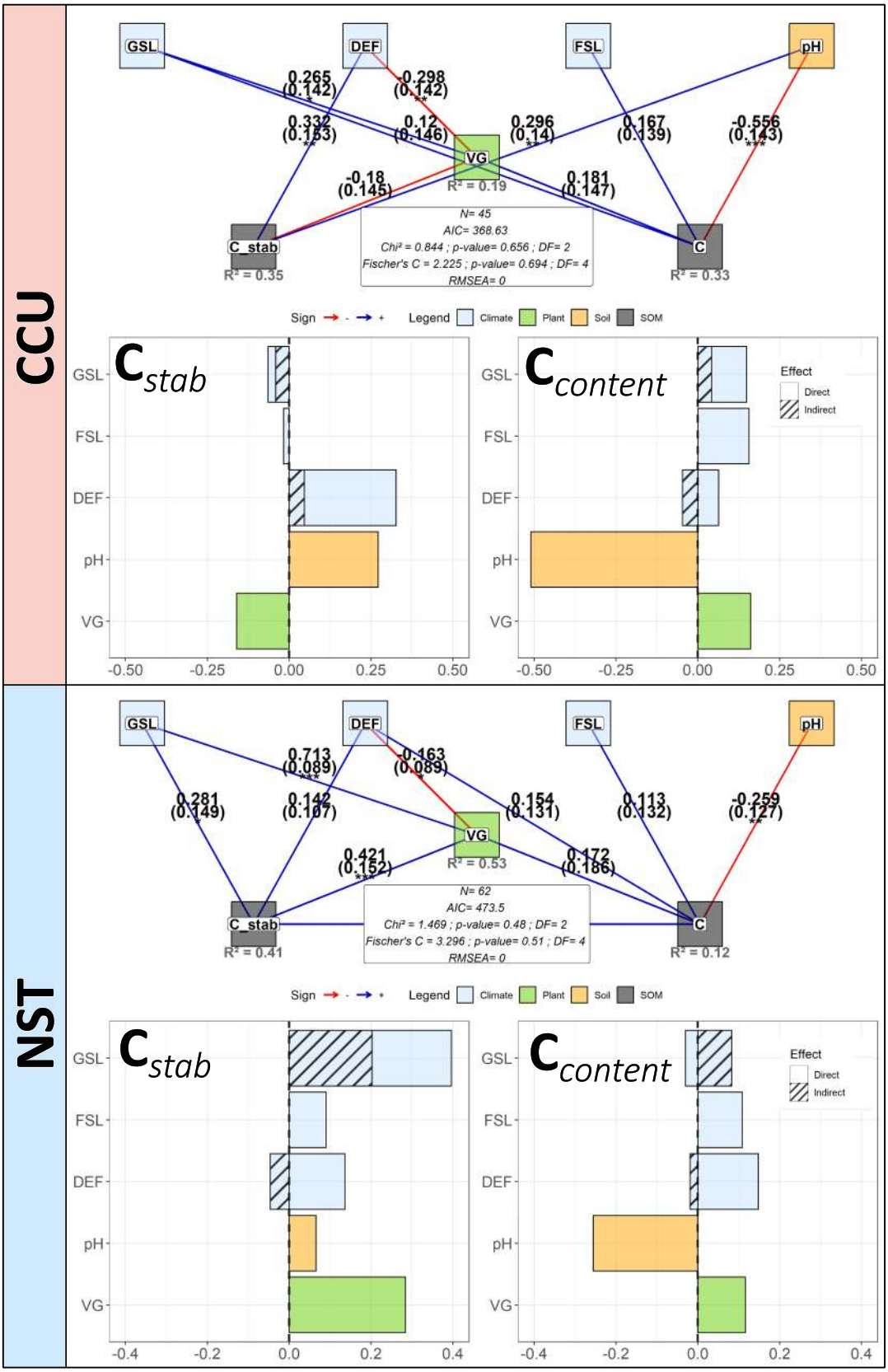


Fig. 4. Structural equation model integrating plant-trait as mediator effect between abiotic variables (climate & pH) and SOC properties. The SEM fit was satisfactory, with RMSEA < 0.01 and P-value from the Chi^2 test $\gg 0.05$. Effect (direct/indirect/total) of each variable in SEM after model bootstrapping was represented in the lower panel for CCU and NST; Model fitting and adjustment were satisfying for both models. GSL = Growing season length; DEF = water deficit; FSL = freezing season length; VG = axis 1 of plant-trait PCA corresponded to conservative-exploitative gradient (Fig. S4.D); C_stab=SOC stability, axis 1 * (−1) of Rock-Eval indices PCA (Fig. S4.B); C=SOC content. Only relations with estimate > 0.1 were presented in plots.

Table 1
Linear mixed model between SOC stability and elevation/FSL, showing that SOC stability was explain both by elevation and mesotopographic gradients (and their interaction).

Formula	Variables	Estimate	P_{value} variables	P_{value} model	R^2 model
——	——	——	——	——	——
	Elevation	−3.075e-03	<0.001 ***		
Cstab~ Elevation* FSL	FSL	−1.060e-01	<0.01 **	<0.001	0.42
	Elevation* FSL	−4.456e-05	<0.01 **	***	
——	——	——	——	——	——

accumulate, such as ridges, the topsoil is exposed to the risk of freezing (Fig. 1.E). These conditions are critical for ecosystem functioning. Our results align with previous studies that highlight the importance of mesotopography in shaping SOC variability. For instance, Patton et al. (2019) found that hillslope curvature (ridge/comb, concave/convex) could account for up to 94 % of TOC variability at a fine scale (see also Fissore et al., (2017); Garcia-Pausas et al., (2007); Zhu et al., (2019). Similar to previous research, we observed greater SOC accumulation in concave areas (with long freezing season length − FSL) than in convex shapes (with short FSL, Fissore et al. (2017), and we found that SOC was less stable on ridges compared to flat slopes (Tian et al., 2020; Zhu et al., 2019a).

SOC properties are influenced by different climatic parameters along the FSL gradient. In the intermediate position (NST), we detected the effect of the elevation gradient: at higher elevations, lower temperatures (GDD, GSL) reduce mineralization more than productivity (see above and Fig. S12). On windy ridges (CCU), we hypothesize that freezing season length slows down microbial activity due to both winter drought (unavailability of frozen water) and cryoturbation from freeze-thaw cycles (causing cell lysis) (Gavazov et al., 2017). Ecosystem functioning is disrupted by frost events, with no buffering effect from the winter season (Ibanez et al., 2021) and no microbial biomass buffer (Brooks et al., 1998), which may result in nutrient loss or unavailability and reduced activity. The reduction in the mineralization period leads to the accumulation of labile SOC. Paradoxically, the longer the freezing season length (FSL), the longer the growing season length (GSL), as a reduced snow cover period allows the GSL to begin earlier. The balance between increased SOC inputs from a longer GSL and decreased winter mineralization due to a longer FSL results in the accumulation of labile SOC, explaining the negative effect of both GSL and FSL on SOC stability (Figs. 3, 4).

For further investigations, SOC should be analyzed in snowbeds (the other half of the gradient, Fig. 1.E). Although SOC content is higher on ridges due to low winter temperatures, this storage occurs mainly near the surface. In snowbeds, SOC mineralization still occurs during the winter (Groffman et al., 2001), leading to greater consumption of biogeochemically labile SOC, resulting in lower SOC contents but with greater biogeochemical stability. Moreover, snowbed soils accumulate erosional deposits (paleosols), which bury SOC (Zhu et al., 2014), and stabilize it through organo-mineral interactions (Kögel-Knabner et al., 2008). Therefore, by considering the entire soil profile, we hypothesize that snowbeds have larger SOC stocks than ridges and that SOC is more stable, as suggested by other studies. For instance, Baptist et al., (2010) demonstrated that decomposition is more intense in areas with late snowmelt than in those with early snowmelt, regardless of litter type (graminoids vs. shrubs). In the same way, Michalet et al. (2002) showed higher SOC stability in snowbed soils than in ridge soils.

4.3. Soil pH

Despite limited variability, soil pH plays a significant role in SOC properties, indicating that the geochemistry of the parent rock and soil type are essential factors. Doetterl et al., (2015) emphasized the impact of lithology (e.g., limestone, granite, basalt, rhyolite) on SOC properties. Here, we suggest that, even within the same rock type (acid rock), slight pH variations can lead to substantial changes in SOC stabilization. The role of pH is twofold: it directly controls microbial community activity (Ibanez et al., 2021; Puissant et al., 2019; Tao et al., 2019), and influences primary productivity, by driving nutrient availability and plant–microbe interactions (Barrow and Hartemink, 2023; Kemmitt et al., 2006; Liu et al., 2021). These findings are in line with Delahaie et al., (2023), who reported positive correlations between soil pH and T50CO2PYR ($r = 0.73$, P-value < 0.001) and negative correlation with HI ($r = -0.42$, P-value < 0.001) in a broad French scale dataset. They suggested that acidity may protect SOM from microbial degradation by reducing microbial activity and SOM mineralization. These findings align with the AMG model, which indicates that mineralization strongly depends on pH, with a significant increase occurring between pH 5.5 and 7 (Clivot et al., 2019).

It should be noted that pH can be related to other stabilization processes, such as organo-mineral interactions, and factors such as grain size (clay content) and the availability of oxyhydroxides (Kögel-Knabner et al., 2008). These characteristics themselves depend on the soil's weathering state, which can also influence pH (Duchaufour et al., 2024; Michalet, 1997). While we ensured some consistency in soil properties by focusing on a single ecosystem type (mountain acidic grasslands), variations in weathering state can still play a significant role, indirectly affecting SOC stability through its influence on other soil characteristics. Moreover, an alternative interpretation of the role of pH should be considered. As proposed by Michalet and Liancourt (2024), and given the narrow range of soil pH variations in our dataset, pH could be a consequence rather than a driver of SOC content. Higher SOC content may lead to greater production of organic acids, resulting in lower soil pH. This interpretation is consistent with the observed negative correlation between SOC content and pH, with correlation coefficients of −0.46 and −0.29 for CCU and NST, respectively (Fig. S13).

4.4. Water regime

The regional water regime is influenced by continentality (Figs. S10 and S11) and elevation. Its interpretation should be approached cautiously. On one hand, it could incorporate spatial autocorrelation, which we aimed to minimize by including 'mountain range' as a random effect. On the other hand, significant uncertainty arises from the coarse resolution of the climate grid used here. Consistent with other studies (Meng et al., 2019), our findings suggest that wetter conditions (high precipitations and high DEF with DEF = PREC − actual evapotranspiration) result in increased SOC concentration. In CCU, DEF (precipitations minus actual evapotranspiration) enhances SOC stability, whereas in NST, DEF generally reduces SOC stability, except through plant-mediated effects (Fig. 4). We propose that SOC stocks and stability are determined by the balance between productivity and mineralization, with their respective increases shaping SOC properties. In both types of grassland, increased productivity contributes to higher SOC stocks. Even with an associated rise in mineralization, it can be assumed that the flux of biogeochemically stable carbon increases with productivity, resulting in net SOC stock growth. In CCU, the increase in productivity under DEF appeared to be smaller than the increase in mineralization, leading to higher SOC stability as the relative proportion of stable carbon increases. Conversely, in NST, the productivity increase under DEF likely exceeded the associated rise in mineralization, resulting in lower SOC stability as the input of labile substrates outpaces the mineralization fluxes.

The interpretation of the water regime must be approached with caution, as it influences various other factors such as pedogenesis, which

in turn affects soil properties like clay content and pH — both of which can impact SOC stability (Michalet and Liancourt, 2024). The water regime itself is governed by the continentality index, which also shapes vegetation distribution as found by Michalet et al., (2021). They demonstrated this relationship in the forests of the northwestern USA, where they quantified rainfall continentality using the Gams angle method. Their findings revealed that rainfall continentality influences ecosystems not only during winter but throughout the year, by affecting nebulosity, temperature, snowfall, and snow cover duration. Further detailed analyses of these parameters on SOC stability could be conducted, particularly at scales relevant to our study, which spans mountain ranges with varying continentality and oceanity indices (see Figs. S10 and S11).

4.5. Plant as mediator of SOC stability

We suggest that climatic conditions, by shaping productivity and resource allocation strategies, affect litter quality inputs (e.g., C:N stoichiometry or oxygen/hydrogen ratios), which in turn impact SOC biogeochemical stability. These findings are in line with previous studies showing that lower productivity tends to increase the C:N ratio of biomass inputs, as poorly productive vegetation may prioritize carbon accumulation for structural material rather than nitrogen-rich growth tissues (Mndela et al., 2022), making SOC more resistant to mineralization (Freppaz et al., 2007, 2006; McLaren and Turkington, 2010).

In CCU, productivity and above-ground biomass were positively correlated with SOC content but negatively correlated with SOC stability. This suggests that the extended growing season length (GSL) in CCU promoted the accumulation of more labile SOC, which was not fully mineralized. SOC content and stability increased with SLA, indicating that poor-quality litter inputs contributed to both SOC accumulation and greater biogeochemical stability. Conversely, in NST, the opposite trend emerged: prolonged GSL appeared to facilitate SOC mineralization. In NST, less stressful conditions enhanced both productivity and SOC mineralization, while, in CCU, harsher conditions resulted in poorer litter quality and higher SOC content, implying that mineralization was significantly constrained.

4.6. Perspectives with climate change

Furthermore, our results highlight the need to better incorporate soil climate, which is strongly related to mesotopographic effects and snow cover duration, into models aimed at spatializing SOC stocks in mountain ecosystems. Predictive distribution of both SOC content and SOC stability will help to anticipate the impact of climate change on SOC stocks.

Our study can be viewed as a space-for-time approach, allowing us to test hypotheses regarding the potential consequences of climate change and setting the stage for further research. Climate models predict shifts in temperature and precipitation regimes (IPCC, 2023), including changes in the rain-snow line. The impact of global warming will depend on the current thermal characteristics of ecosystems, which suggests that sensitivity to climate change is more complex than just considering changes in mean annual temperature. CCU grasslands appear more vulnerable to alterations in the water regime. Areas currently experiencing high DEF and low GDD may change towards functioning similar to ecosystems with lower DEF and higher GDD, potentially resulting in carbon loss (Fig. S12). In contrast, NST grasslands could respond in two opposite ways (Choler (2005), Fig. S12). SOC at higher elevations seems particularly vulnerable to global warming, as it is biogeochemically labile and stabilized by low temperatures. This makes it susceptible to environments with higher GDD, suggesting a shift towards lower-elevation dynamics and associated carbon losses (Fig. S12). However, NST thermal conditions could also evolve towards those of CCU, where snow cover duration declines (Notarnicola, 2020; Rumpf et al., 2022), leading to more frequent winter soil freezing and reduced mineralization activity. These hypotheses point to the need for future studies focused on: i) the effects of snow deficits on SOC in intermediate grasslands, and ii) the impact of warming on SOC properties, such as increased GDD and extended GSL (Khedim et al., 2023).

5. Conclusion

To conclude, our results underscore the significant biogeochemical lability of SOC in mountain grasslands, indicating substantial accumulation due to low temperatures. We observed a notable influence of microclimate conditions on SOC properties. Specifically, lower temperatures were associated with increased SOC content and decreased SOC stability. Temperatures decrease results from both higher elevation and reduced snow cover duration (which diminishes insulation). In windy ridges, longer growing seasons combined with more intense soil freezing during winter led to higher SOC lability. Conversely, in intermediate positions, a longer growing season enhanced SOC stability by promoting increased decomposition activity. These findings provide space-for-time insights regarding how SOC properties might shift with climate change, considering both rising temperatures and changes in snow cover duration.

CRediT authorship contribution statement

Nicolas Bonfanti: Writing – original draft, Investigation, Formal analysis, Data curation. **Jérôme Poulenard:** Writing – review & editing, Validation, Supervision, Investigation. **Jean-Christophe Clément:** Writing – review & editing, Validation, Supervision. **Pierre Barré:** Writing – review & editing, Validation, Supervision, Methodology, Conceptualization. **François Baudin:** Writing – review & editing, Validation, Methodology, Investigation. **Pavel Dan Turtureanu:** Writing – review & editing, Validation, Project administration, Funding acquisition, Conceptualization. **Mihai Pușcaș:** Writing – review & editing, Validation, Methodology, Funding acquisition, Conceptualization. **Amélie Saillard:** Resources, Investigation. **Pablo Raguet:** Writing – review & editing, Visualization, Data curation. **Bogdan-Iuliu Hurdu:** Resources, Investigation, Conceptualization. **Philippe Choler:** Writing – review & editing, Validation, Supervision, Resources, Project administration, Methodology, Funding acquisition, Conceptualization.

Declaration of competing interest

The authors declare that they have no known competing financial interests or personal relationships that could have appeared to influence the work reported in this paper.

Acknowledgements

This study was supported by the ODYSSEE project (ANR-13-ISV7-0004, PN-II-ID-JRP-RO-FR-2012) and BioDivMount project (BRANCUSI No. 32660WB and PN-II-CT-ROFR-2014-2-0011), funded by ANR France and UEFISCDI Romania. Thanks are due to Olivier Tarpin, Maxime Bouclier, Lambert Bourdenet, Andriy Novikov and Jozef Šibíke for helping with the field work and to Stanislav Březina, Irena Hubálková (Krkonoše Mountains National Park) and Jindrich Chlapek (Jeseníky Protected Landscape Area) for facilitating the access to study sites and assistance in the field. We are grateful to the administrations of Central Balkan National Park and Mercantour National Park for granting access to several sites. Additionally, we express our warm thanks to Krahulec František and Patrik Mráz for their advice, and for their help in gathering literature and field data. Florence Savignac is acknowledged for her help during Rock-Eval analyses.

Appendix A. Supplementary data

Supplementary data to this article can be found online at https://doi.

org/10.1016/j.catena.2025.108744.

References

Abatzoglou, J.T., Dobrowski, S.Z., Parks, S.A., Hegewisch, K.C., 2018. TerraClimate, a high-resolution global dataset of monthly climate and climatic water balance from 1958–2015. Sci Data 5, 1–12. https://doi.org/10.1038/sdata.2017.191.

Amelung, W., Brodowski, S., Sandhage-Hofmann, A., Bol, R., 2008. Chapter 6 combining biomarker with stable isotope analyses for assessing the transformation and turnover of soil organic matter. In: Advances in Agronomy. Academic Press, pp. 155–250, 10.1016/S0065-2113(08)00606-8.

Andersson, S., Nilsson, S.I., 2001. Influence of ph and temperature on microbial activity, substrate availability of soil-solution bacteria and leaching of dissolved organic carbon in a mor humus. Soil Biology 11.

Balesdent, J., Besnard, E., Arrouays, D., Chenu, C., 1998. The dynamics of carbon in particle size fractions of soil in a forest cultivated sequence. Plant and Soil 201, 49–57. https://doi.org/10.1023/A:1004337314970.

Baptist, F., Yoccoz, N.G., Choler, P., 2010. Direct and indirect control by snow cover over decomposition in alpine tundra along a snowmelt gradient. Plant Soil 328, 397–410. https://doi.org/10.1007/s11104-009-0119-6.

Barré, P., Plante, A., Cécillon, L., Lutfalla, S., Baudin, F., Bernard, S., Christensen, B., Eglin, T., Fernandez, J., Houot, S., Kätterer, T., Guillou, C., Macdonald, A., Oort, F., Chenu, C., 2016. The energetic and chemical signatures of persistent soil organic matter. Biogeochemistry 130, 1–12. https://doi.org/10.1007/s10533-016-0246-0.

Barré, P., Cécillon, L., Kanari, E., 2023. Characterization and evaluation of the stability of soil organic matter. In: The Rock-Eval Method. John Wiley & Sons Ltd, pp. 181–207, 10.1002/9781394256235.ch10.

Barrow, N.J., Hartemink, A.E., 2023. The effects of pH on nutrient availability depend on both soils and plants. Plant Soil 487, 21–37. https://doi.org/10.1007/s11104-023-05960-5.

Bates, D., Mächler, M., Bolker, B., Walker, S., 2015. Fitting linear mixed-effects models using **lme4**. J. Stat. Soft. 67. https://doi.org/10.18637/jss.v067.i01.

Bernard, L., Foulquier, A., Gallet, C., Lavorel, S., Clément, J.-C., 2019. Effects of snow pack reduction and drought on litter decomposition in subalpine grassland communities. Plant Soil 435, 225–238. https://doi.org/10.1007/s11104-018-3891-3.

Bernoux, M., Cerri, C.C., Neill, C., de Moraes, J.F.L., 1998. The use of stable carbon isotopes for estimating soil organic matter turnover rates. Geoderma 82, 43–58. https://doi.org/10.1016/S0016-7061(97)00096-7.

Braun-Blanquet, J., 1964. Pflanzensoziologie. Grundzüge der Vegetationskunde.

Brooks, P., Williams, M., Schmidt, S., 1998. Inorganic nitrogen and microbial biomass dynamics before and during spring snowmelt. Biogeochemistry 43, 1–15. https://doi.org/10.1023/A:1005947511910.

Browne, M.W., Cudeck, R., 1992. Alternative ways of assessing model fit. Sociol. Methods Res. 21, 230–258. https://doi.org/10.1177/0049124192021002005.

Buckeridge, K.M., Grogan, P., 2010. Deepened snow increases late thaw biogeochemical pulses in mesic low arctic tundra. Biogeochemistry 101, 105–121. https://doi.org/10.1007/s10533-010-9426-5.

Budge, K., Leifeld, J., Hiltbrunner, E., Fuhrer, J., 2011. Alpine grassland soils contain large proportion of labile carbon but indicate long turnover times. Biogeosciences 8, 1911–1923. https://doi.org/10.5194/bg-8-1911-2011.

Buyanovsky, G.A., Aslam, M., Wagner, G.H., 1994. Carbon turnover in soil physical fractions. Soil Sci. Soc. Am. J. 58, 1167–1173. https://doi.org/10.2136/sssaj1994.03615995005800040023x.

Calcagno, V., Calcagno, M.V., Java, S., Suggests, M., 2020. Package 'glmulti.' Model Selection and Multimodel Inference Made Easy. Version 1.

Cécillon, L., Baudin, F., Chenu, C., Houot, S., Jolivet, R., Kätterer, T., Lutfalla, S., Macdonald, A., van Oort, F., Plante, A.F., Savignac, F., Soucémarianadin, L.N., Barré, P., 2018. A model based on Rock-Eval thermal analysis to quantify the size of the centennially persistent organic carbon pool in temperate soils. Biogeosciences 15, 2835–2849. https://doi.org/10.5194/bg-15-2835-2018.

Cécillon, L., Baudin, F., Chenu, C., Christensen, B.T., Franko, U., Houot, S., Kanari, E., Kätterer, T., Merbach, I., van Oort, F., Poeplau, C., Quezada, J.C., Savignac, F., Soucémarianadin, L.N., Barré, P., 2021. Partitioning soil organic carbon into its centennially stable and active fractions with machine-learning models based on Rock-Eval® thermal analysis (PARTYSOCv2.0 and.

Choler, P., 2005. Consistent shifts in alpine plant traits along a mesotopographical gradient. Arct. Antarct. Alp. Res. 37, 444–453. https://doi.org/10.1657/1523-0430(2005)037[0444:CSIAPT]2.0.CO;2.

Choler, P., 2015. Growth response of temperate mountain grasslands to inter-annual variations in snow cover duration. Biogeosciences 12, 3885–3897. https://doi.org/10.5194/bg-12-3885-2015.

Choler, P., 2023. Above-treeline ecosystems facing drought: lessons from the 2022 European summer heat wave. Biogeosciences 20, 4259–4272. https://doi.org/10.5194/bg-20-4259-2023.

Choler, P., Bayle, A., Carlson, B.Z., Randin, C., Filippa, G., Cremonese, E., 2021. The tempo of greening in the European Alps: spatial variations on a common theme. Glob. Chang. Biol. 27, 5614–5628. https://doi.org/10.1111/gcb.15820.

Clément, J.C., Robson, T.M., Guillemin, R., Barre, P., Lochet, J., Aubert, S., Lavorel, S., Saccone, P., Lochet, J., Aubert, S., Lavorel, S., Aubert, S., Robson, T.M., Guillemin, R., 2012. The effects of snow-N deposition and snowmelt dynamics on soil-N cycling in marginal terraced grasslands in the French Alps. Biogeochemistry.

Clivot, H., Mouny, J.-C., Duparque, A., Dinh, J.-L., Denoroy, P., Houot, S., Vertès, F., Trochard, R., Bouthier, A., Sagot, S., Mary, B., 2019. Modeling soil organic carbon evolution in long-term arable experiments with AMG model. Environ. Model. Softw. 118, 99–113. https://doi.org/10.1016/j.envsoft.2019.04.004.

Davidson, E.A., Janssens, I.A., 2006. Temperature sensitivity of soil carbon decomposition and feedbacks to climate change. Nature 440, 165–173. https://doi.org/10.1038/nature04514.

De Frenne, P., Rodríguez-Sánchez, F., Coomes, D.A., Baeten, L., Verstraeten, G., Vellend, M., Bernhardt-Römermann, M., Brown, C.D., Brunet, J., Cornelis, J., Decocq, G.M., Dierschke, H., Eriksson, O., Gilliam, F.S., Hédl, R., Heinken, T., Hermy, M., Hommel, P., Jenkins, M.A., Kelly, D.L., Kirby, K.J., Mitchell, F.J.G., Naaf, T., Newman, M., Peterken, G., Petřík, P., Schultz, J., Sonnier, G., Van Calster, H., Waller, D.M., Walther, G.-R., White, P.S., Woods, K.D., Wulf, M., Graae, B.J., Verheyen, K., 2013. Microclimate moderates plant responses to macroclimate warming. Proc. Natl. Acad. Sci. 110, 18561–18565. https://doi.org/10.1073/pnas.1311190110.

Delahaie, A.A., Barré, P., Baudin, F., Arrouays, D., Bispo, A., Boulonne, L., Chenu, C., Jolivet, C., Martin, M.P., Ratié, C., Saby, N.P.A., Savignac, F., Cécillon, L., 2023. Elemental stoichiometry and Rock-Eval® thermal stability of organic matter in French topsoils. SOIL 9, 209–229. https://doi.org/10.5194/soil-9-209-2023.

Derrien, D., Dignac, M.F., Basile-Doelsch, I., Barot, S., Cécillon, L., Chenu, C., Chevallier, T., Freschet, G.T., Garnier, P., Guenet, B., Hedde, M., Klumpp, K., Lashermes, G., Maron, P.A., Nunan, N., Roumet, C., Baré, P., 2016. Stocker du C dans les sols : quels mécanismes, quelles pratiques agricoles, quels indicateurs ? Etude et Gestion des Sols 32.

Disnar, J.R., Guillet, B., Keravis, D., Di-Giovanni, C., Sebag, D., 2003. Soil organic matter (SOM) characterization by Rock-Eval pyrolysis: scope and limitations. Org Geochem. 34, 327–343. https://doi.org/10.1016/S0146-6380(02)00239-5.

Djukic, I., Zehetner, F., Tatzber, M., Gerzabek, M.H., 2010. Soil organic-matter stocks and characteristics along an Alpine elevation gradient. Z. Pflanzenernähr. Bodenk. 173, 30–38. https://doi.org/10.1002/jpln.200900027.

Doetterl, S., Stevens, A., Six, J., Merckx, R., Van Oost, K., Casanova Pinto, M., Casanova-Katny, A., Muñoz, C., Boudin, M., Zagal Venegas, E., Boeckx, P., 2015. Soil carbon storage controlled by interactions between geochemistry and climate. Nature Geosci 8, 780–783. https://doi.org/10.1038/ngeo2516.

Dorji, T., Field, D.J., Odeh, I.O.A., 2020. Soil aggregate stability and aggregate-associated organic carbon under different land use or land cover types. Soil Use Manag. 36, 308–319. https://doi.org/10.1111/sum.12549.

Dray, S., Dufour, A.-B., Thioulouse, and J., Jombart, with contributions from T., Pavoine, S., Lobry, J.R., Ollier, S., Borcard, D., Legendre, P., Chessel, S.B. and A.S.B. on earlier work by D., 2023. ade4: Analysis of Ecological Data: Exploratory and Euclidean Methods in Environmental Sciences.

Duchaufour, P., Faivre, P., Poulenard, J., Gury, M., 2024. Introduction à la science du sol, Dunod (8e édition). ed.

EEA, E.E.A., 2024. European Climate Risk Assessment (Publication No. 01/2024).

Fick, S., Hijmans, R., 2017. WorldClim 2: New 1-km spatial resolution climate surfaces for global land areas. Int. J. Climatol. 37. https://doi.org/10.1002/joc.5086.

Fissore, C., Dalzell, B.J., Berhe, A.A., Voegtle, M., Evans, M., Wu, A., 2017. Influence of topography on soil organic carbon dynamics in a Southern California grassland. Catena 149, 140–149. https://doi.org/10.1016/j.catena.2016.09.016.

Freppaz, M., Williams, B., Edwards, A., Scalenghe, R., Zanini, E., 2006. Labile nitrogen, carbon, and phosphorus pools and nitrogen mineralization and immobilization rates at low temperatures in seasonally snow-covered soils. Biol. Fertil. Soils 43, 519–529. https://doi.org/10.1007/s00374-006-0130-5.

Freppaz, M., Williams, B.L., Edwards, A.C., Scalenghe, R., Zanini, E., 2007. Simulating soil freeze/thaw cycles typical of winter alpine conditions: Implications for N and P availability. Appl. Soil Ecol. 35, 247–255. https://doi.org/10.1016/j.apsoil.2006.03.012.

Garcia-Pausas, J., Casals, P., Camarero, L., Huguet, C., Sebastià, M.-T., Thompson, R., Romanyà, J., 2007. Soil organic carbon storage in mountain grasslands of the pyrenees: effects of climate and topography. Biogeochemistry 82, 279–289.

Garcia-Pausas, J., Casals, P., Rovira, P., Vallecillo, S., Sebastià, M.-T., Romanyà, J., 2012. Decomposition of labelled roots and root-C and -N allocation between soil fractions in mountain grasslands. Soil Biol. Biochem. 49, 61–69. https://doi.org/10.1016/j.soilbio.2012.02.015.

Garnier, E., Shipley, B., Roumet, C., Laurent, G., 2001. A standardized protocol for the determination of specific leaf area and leaf dry matter content. Funct. Ecol. 15, 688–695. https://doi.org/10.1046/j.0269-8463.2001.00563.x.

Gavazov, K., Ingrisch, J., Hasibeder, R., Mills, R.T.E., Buttler, A., Gleixner, G., Pumpanen, J., Bahn, M., 2017. Winter ecology of a subalpine grassland: effects of snow removal on soil respiration, microbial structure and function. Sci. Total Environ. 590–591, 316–324. https://doi.org/10.1016/j.scitotenv.2017.03.010.

Gennai, M., Foggi, B., Viciani, D., Carbognani, M., Tomaselli, M., 2014. The Nardus-rich communities in the Northern Apennines (N-Italy): a phytosociological, ecological and phytogeographical study. Phytocoenologia 44, 55–80. https://doi.org/10.1127/0340-269X/2014/0044-0574.

Geremia, R.A., Puşcaş, M., Zinger, L., Bonneville, J.-M., Choler, P., 2016. Contrasting microbial biogeographical patterns between anthropogenic subalpine grasslands and natural alpine grasslands. New Phytol. 209, 1196–1207. https://doi.org/10.1111/nph.13690.

Grace, J.B., 2006. Structural equation modeling and natural systems. Cambridge University Press.

Gregorich, E.G., Gillespie, A.W., Beare, M.H., Curtin, D., Sanei, H., Yanni, S.F., 2015. Evaluating biodegradability of soil organic matter by its thermal stability and chemical composition. Soil Biol. Biochem. 91, 182–191. https://doi.org/10.1016/j.soilbio.2015.08.032.

Grime, J.P., 1998. Benefits of plant diversity to ecosystems: immediate, filter and founder effects. J. Ecol. 86, 902–910. https://doi.org/10.1046/j.1365-2745.1998.00306.x.

Groffman, P.M., Driscoll, C.T., Fahey, T.J., Hardy, J.P., Fitzhugh, R.D., Tierney, G.L., 2001. Colder soils in a warmer world: A snow manipulation study in a northern hardwood forest ecosystem 16.
Guidi, C., Vesterdal, L., Gianelle, D., Rodeghiero, M., 2014. Changes in soil organic carbon and nitrogen following forest expansion on grassland in the Southern Alps. For. Ecol. Manage. 328, 103–116. https://doi.org/10.1016/j.foreco.2014.05.025.
Hafner, S., Unteregelsbacher, S., Seeber, E., Lena, B., Xu, X., Li, X., Guggenberger, G., Miehe, G., Kuzyakov, Y., 2012. Effect of grazing on carbon stocks and assimilate partitioning in a Tibetan montane pasture revealed by 13CO2 pulse labeling. Glob Change Biol 18, 528–538. https://doi.org/10.1111/j.1365-2486.2011.02557.x.
Heckman, K., Welty-Bernard, A., Rasmussen, C., Schwartz, E., 2009. Geologic controls of soil carbon cycling and microbial dynamics in temperate conifer forests. Chem. Geol. 267, 12–23. https://doi.org/10.1016/j.chemgeo.2009.01.004.
Hilton, R.G., Galy, V., Gaillardet, J., Dellinger, M., Bryant, C., O'Regan, M., Gröcke, D.R., Coxall, H., Bouchez, J., Calmels, D., 2015. Erosion of organic carbon in the Arctic as a geological carbon dioxide sink. Nature 524, 84–87. https://doi.org/10.1038/nature14653.
Ibanez, S., Brun, C., Millery, A., Piton, G., Bernard, L., Avrillier, J.-N., Gallet, C., Foulquier, A., Clément, J.-C., 2021. Litter and soil characteristics mediate the buffering effect of snow cover on litter decomposition. Plant Soil 460, 511–525. https://doi.org/10.1007/s11104-020-04803-x.
IPCC, 2023. Contribution of Working Groups I, II and III to the Sixth Assessment Report of the Intergovernmental Panel on Climate Change.
Jaeger, B., 2017. r2glmm: Computes R Squared for Mixed (Multilevel) Models.
Jin, H., Ma, Q., 2021. Impacts of permafrost degradation on carbon stocks and emissions under a warming climate: a review. Atmos. 12, 1425. https://doi.org/10.3390/atmos12111425.
Jöreskog, K.G., Sörbom, D., 1993. LISREL 8: structural equation modeling with the SIMPLIS command language. Scientific Software International.
Jusselme, M.-D., Saccone, P., Zinger, L., Faure, M., Le Roux, X., Guillaumaud, N., Bernard, L., Clement, J.-C., Poly, F., 2016. Variations in snow depth modify N-related soil microbial abundances and functioning during winter in subalpine grassland. Soil Biol. Biochem. 92, 27–37. https://doi.org/10.1016/j.soilbio.2015.09.013.
Kemmitt, S.J., Wright, D., Goulding, K.W.T., Jones, D.L., 2006. pH regulation of carbon and nitrogen dynamics in two agricultural soils. Soil Biol. Biochem. 38, 898–911. https://doi.org/10.1016/j.soilbio.2005.08.006.
Kemppinen, J., Lembrechts, J.J., Van Meerbeek, K., Carnicer, J., Chardon, N.I., Kardol, P., Lenoir, J., Liu, D., Maclean, I., Pergl, J., Saccone, P., Senior, R.A., Shen, T., Słowińska, S., Vandvik, V., von Oppen, J., Aalto, J., Ayalew, B., Bates, O., Bertelsmeier, C., Bertrand, R., Beugnon, R., Borderieux, J., Brůna, J., Buckley, L., Bujan, J., Casanova-Katny, A., Christiansen, D.M., Collart, F., De Lombaerde, E., De Pauw, K., Depauw, L., Di Musciano, M., Díaz Borrego, R., Díaz-Calafat, J., Ellis-Soto, D., Esteban, R., de Jong, G.F., Gallois, E., Garcia, M.B., Gillerot, L., Greiser, C., Gril, E., Haesen, S., Hampe, A., Hedwall, P.-O., Hes, G., Hespanhol, H., Hoffrén, R., Hylander, K., Jiménez-Alfaro, B., Jucker, T., Klinges, D., Kolstela, J., Kopecký, M., Kovács, B., Maeda, E.E., Máliš, F., Man, M., Mathiak, C., Meineri, E., Naujokaitis-Lewis, I., Nijs, I., Normand, S., Nuñez, M., Orczewska, A., Peña-Aguilera, P., Pincebourde, S., Plichta, R., Quick, S., Renault, D., Ricci, L., Rissanen, T., Segura-Hernández, L., Selvi, F., Serra-Diaz, J.M., Soifer, L., Spicher, F., Svenning, J.-C., Tamian, A., Thomaes, A., Thoonen, M., Trew, B., Van de Vondel, S., van den Brink, L., Vangansbeke, P., Verdonck, S., Vitkova, M., Vives-Ingla, M., von Schmalensee, L., Wang, R., Wild, J., Williamson, J., Zellweger, F., Zhou, X., Zuza, E. J., De Frenne, P., 2024. Microclimate, an important part of ecology and biogeography. Glob. Ecol. Biogeogr. 33, e13834. https://doi.org/10.1111/geb.13834.
Khedim, N., Cécillon, L., Poulenard, J., Barré, P., Baudin, F., Marta, S., Rabatel, A., Dentant, C., Cauvy-Fraunié, S., Anthelme, F., Gielly, L., Ambrosini, R., Franzetti, A., Azzoni, R.S., Caccianiga, M.S., Compostella, C., Clague, J., Tielidze, L., Messager, E., Choler, P., Ficetola, G.F., 2021. Topsoil organic matter build-up in glacier forelands around the world. Glob. Chang. Biol. 27, 1662–1677. https://doi.org/10.1111/gcb.15496.
Khedim, N., Jérôme, P., Lauric, C., François, B., Pierre, B., Amélie, S., Bektaş, B., Karl, G., Sandra, L., Tamara, M., Philippe, C., 2023. Soil organic matter changes under experimental pedoclimatic modifications in mountain grasslands of the French Alps. Geoderma 429, 116238. https://doi.org/10.1016/j.geoderma.2022.116238.
Kögel-Knabner, I., Guggenberger, G., Kleber, M., Kandeler, E., Kalbitz, K., Scheu, S., Eusterhues, K., Leinweber, P., 2008. Organo-mineral associations in temperate soils: Integrating biology, mineralogy, and organic matter chemistry. J. Plant Nutr. Soil Sci. 171, 61–82. https://doi.org/10.1002/jpln.200700048.
Laub, M., Demyan, M.S., Nkwain, Y.F., Blagodatsky, S., Kätterer, T., Piepho, H.-P., Cadisch, G., 2020. DRIFTS band areas as measured pool size proxy to reduce parameter uncertainty in soil organic matter models. Biogeosciences 17, 1393–1413. https://doi.org/10.5194/bg-17-1393-2020.
Lavallee, J.M., Soong, J.L., Cotrufo, M.F., 2020. Conceptualizing soil organic matter into particulate and mineral-associated forms to address global change in the 21st century. Glob. Chang. Biol. 26, 261–273. https://doi.org/10.1111/gcb.14859.
Lê, S., Josse, J., Husson, F., 2008. FactoMineR: an R package for multivariate analysis. J. Stat. Soft. 25. https://doi.org/10.18637/jss.v025.i01.
Lefcheck, J., Byrnes, J., Grace, J., 2023. piecewiseSEM: Piecewise Structural Equation Modeling.
Leifeld, J., Zimmermann, M., Fuhrer, J., Conen, F., 2009. Storage and turnover of carbon in grassland soils along an elevation gradient in the Swiss Alps. Glob. Chang. Biol. 15, 668–679. https://doi.org/10.1111/j.1365-2486.2008.01782.x.
Li, Y., Dong, S., Liu, S., Zhou, H., Gao, Q., Cao, G., Wang, X., Su, X., Zhang, Y., Tang, L., Zhao, H., Wu, X., 2015. Seasonal changes of CO2, CH4 and N2O fluxes in different types of alpine grassland in the Qinghai-Tibetan Plateau of China. Soil Biol. Biochem. 80, 306–314. https://doi.org/10.1016/j.soilbio.2014.10.026.
Li, X., McCarty, G.W., Karlen, D.L., Cambardella, C.A., 2018. Topographic metric predictions of soil redistribution and organic carbon in Iowa cropland fields. Catena 160, 222–232. https://doi.org/10.1016/j.catena.2017.09.026.
Liu, J.-J., Xu, Y., Shan, Y.-X., Burgess, K.S., Ge, X.-J., 2021. Biotic and abiotic factors determine species diversity–productivity relationships in mountain meadows. J. Plant Ecol. 14, 1175–1188. https://doi.org/10.1093/jpe/rtab064.
Lorenz, K., Lal, R., Preston, C.M., Nierop, K.G.J., 2007. Strengthening the soil organic carbon pool by increasing contributions from recalcitrant aliphatic bio(macro) molecules. Geoderma 142, 1–10. https://doi.org/10.1016/j.geoderma.2007.07.013.
McLaren, J.R., Turkington, R., 2010. Plant functional group identity differentially affects leaf and root decomposition. Glob. Chang. Biol. 16, 3075–3084. https://doi.org/10.1111/j.1365-2486.2009.02151.x.
Meng, Z., Mengxu, Z., Liu, W., Deo, R., Zhang, C., Yang, L., 2019. Soil organic carbon in semiarid alpine regions: the spatial distribution, stock estimation, and environmental controls. J. Soil. Sediment. https://doi.org/10.1007/s11368-019-02295-6.
Michalet, R., 1997. Fractionnement de la matière organique dans les sols forestiers des montagnes calcaires du Maroc. Coll. IHSS : Les substances humiques dans l'environnement, Toulouse (France). Novembre 1996, 17–28.
Michalet, R., Gandoy, C., Joud, D., Pagès, J.-P., Choler, P., 2002. Plant community composition and biomass on calcareous and siliceous substrates in the northern french alps: comparative effects of soil chemistry and water status. Arct. Antarct. Alp. Res. 34, 102–113. https://doi.org/10.1080/15230430.2002.12003474.
Michalet, R., Choler, P., Callaway, R.M., Whitham, T.G., 2021. Rainfall continentality, via the winter Gams angle, provides a new dimension to biogeographical distributions in the western United States. Global Ecol. Biogeogr. 30, 384–397. https://doi.org/10.1111/geb.13223.
Michalet, R., Liancourt, P., 2024. The interplay between climate and bedrock type determines litter decomposition in temperate forest ecosystems. Soil Biol. Biochem. 195, 109476. https://doi.org/10.1016/j.soilbio.2024.109476.
Mndela, M., Tjelele, J.T., Madakadze, I.C., Mangwane, M., Samuels, I.M., Muller, F., Pule, H.T., 2022. A global meta-analysis of woody plant responses to elevated CO2: implications on biomass, growth, leaf N content, photosynthesis and water relations. Ecol. Process. 11, 52. https://doi.org/10.1186/s13717-022-00397-7.
Moni, C., Chabbi, A., Nunan, N., Rumpel, C., Chenu, C., 2010. Spatial dependance of organic carbon–metal relationships. Geoderma 158, 120–127. https://doi.org/10.1016/j.geoderma.2010.04.014.
Notarnicola, C., 2020. Hotspots of snow cover changes in global mountain regions over 2000–2018. Remote Sens. Environ. 243, 111781. https://doi.org/10.1016/j.rse.2020.111781.
Ozenda, P., 1985. La vegetation de la chaine alpine dans l' espace montagnard europeen., FAO. ed.
Patton, N.R., Lohse, K.A., Seyfried, M.S., Godsey, S.E., Parsons, S.B., 2019. Topographic controls of soil organic carbon on soil-mantled landscapes. Sci Rep 9, 6390. https://doi.org/10.1038/s41598-019-42556-5.
Plante, A.F., Fernández, J.M., Haddix, M.L., Steinweg, J.M., Conant, R.T., 2011. Biological, chemical and thermal indices of soil organic matter stability in four grassland soils. Soil Biol. Biochem. 43, 1051–1058. https://doi.org/10.1016/j.soilbio.2011.01.024.
Puissant, J., Briony, J., Goodall, T., Mang, D., Blaud, A., Gweon, H.S., Malik, A., Jones, D. L., Clark, I.M., Hirsch, P.R., Griffiths, R., 2019. The pH optimum of soil exoenzymes adapt to long term changes in soil pH. Soil Biol. Biochem. 138, 107601. https://doi.org/10.1016/j.soilbio.2019.107601.
Puşcaş, M., Choler, P., 2012. A biogeographic delineation of the European Alpine System based on a cluster analysis of Carex curvula-dominated grasslands. Flora - Morphology, Distribution, Functional Ecology of Plants 207, 168–178. https://doi.org/10.1016/j.flora.2012.01.002.
RMQS, 2017. La carte nationale des stocks de carbone des sols intégrée dans la carte mondiale de la FAO - Martin Manuel - GIS Sol. Doi: 10.15454/JCONRJ.
Rumpf, S.B., Gravey, M., Brönnimann, O., Luoto, M., Cianfrani, C., Mariethoz, G., Guisan, A., 2022. From white to green: Snow cover loss and increased vegetation productivity in the European Alps. Science 376, 1119–1122. https://doi.org/10.1126/science.abn6697.
Saccone, P., Morin, S., Baptist, F., Bonneville, J.-M., Colace, M.-P., Domine, F., Faure, M., Geremia, R., Lochet, J., Poly, F., Lavorel, S., Clément, J.-C., 2013. The effects of snowpack properties and plant strategies on litter decomposition during winter in subalpine meadows. Plant Soil 363, 215–229. https://doi.org/10.1007/s11104-012-1307-3.
Saenger, A., Cécillon, L., Poulenard, J., Bureau, F., De Daniéli, S., Gonzalez, J.-M., Brun, J.-J., 2015. Surveying the carbon pools of mountain soils: A comparison of physical fractionation and Rock-Eval pyrolysis. Geoderma 241–242, 279–288. https://doi.org/10.1016/j.geoderma.2014.12.001.
Schimel, J.P., Schaeffer, S.M., 2012. Microbial control over carbon cycling in soil. Front. Microbio. 3. https://doi.org/10.3389/fmicb.2012.00348.
Schinner, F., 1982. Soil microbial activities and litter decomposition related to altitude. Plant Soil 65, 87–94. https://doi.org/10.1007/BF02376806.
Schlag, R.N., Erschbamer, B., 2000. Germination and establishment of seedlings on a glacier foreland in the central alps, Austria. Arct. Antarct. Alp. Res. 32, 270–277. https://doi.org/10.1080/15230430.2000.12003364.
Schmidt, M.W.I., Torn, M.S., Abiven, S., Dittmar, T., Guggenberger, G., Janssens, I.A., Kleber, M., Kögel-Knabner, I., Lehmann, J., Manning, D.A.C., Nannipieri, P., Rasse, D.P., Weiner, S., Trumbore, S.E., 2011. Persistence of soil organic matter as an ecosystem property. Nature 478, 49–56. https://doi.org/10.1038/nature10386.

Schuur, E.A.G., Bockheim, J., Canadell, J.G., Euskirchen, E., Field, C.B., Goryachkin, S. V., Hagemann, S., Kuhry, P., Lafleur, P.M., Lee, H., Mazhitova, G., Nelson, F.E., Rinke, A., Romanovsky, V.E., Shiklomanov, N., Tarnocai, C., Venevsky, S., Vogel, J. G., Zimov, S.A., 2008. Vulnerability of permafrost carbon to climate change: implications for the global carbon cycle. Bioscience 58, 701–714. https://doi.org/10.1641/B580807.

Sebag, D., Verrecchia, E.P., Cécillon, L., Adatte, T., Albrecht, R., Aubert, M., Bureau, F., Cailleau, G., Copard, Y., Decaens, T., Disnar, J.-R., Hetényi, M., Nyilas, T., Trombino, L., 2016. Dynamics of soil organic matter based on new Rock-Eval indices. Geoderma 284, 185–203. https://doi.org/10.1016/j.geoderma.2016.08.025.

Siewert, M.B., Hanisch, J., Weiss, N., Kuhry, P., Maximov, T.C., Hugelius, G., 2015. Comparing carbon storage of Siberian tundra and taiga permafrost ecosystems at very high spatial resolution. J. Geophys. Res. Biogeo. 120, 1973–1994. https://doi.org/10.1002/2015JG002999.

Silver, W.L., Miya, R.K., 2001. Global patterns in root decomposition: comparisons of climate and litter quality effects. Oecologia 129, 407–419. https://doi.org/10.1007/s004420100740.

SoDa, 2015. HelioClim-1 monthly, weekly and daily Global Solar Irradiation values over a horizontal plane [WWW Document]. SoDa. URL https://www.soda-pro.com (accessed 3.23.23).

Soucémarianadin, L., Cécillon, L., Chenu, C., Baudin, F., Nicolas, M., Girardin, C., Barré, P., 2018. Is Rock-Eval 6 thermal analysis a good indicator of soil organic carbon lability? – A method-comparison study in forest soils. Soil Biol. Biochem. 117, 108–116. https://doi.org/10.1016/j.soilbio.2017.10.025.

Stephenson, N., 1998. Actual evapotranspiration and deficit: biologically meaningful correlates of vegetation distribution across spatial scales. J. Biogeogr. 25, 855–870. https://doi.org/10.1046/j.1365-2699.1998.00233.x.

Tao, J., Zuo, J., He, Z., Wang, Y., Liu, J., Liu, W., Cornelissen, J.H.C., 2019. Traits including leaf dry matter content and leaf pH dominate over forest soil pH as drivers of litter decomposition among 60 species. Funct. Ecol. 33, 1798–1810. https://doi.org/10.1111/1365-2435.13413.

Tian, Q., Wang, D., Li, D., Huang, L., Wang, M., Liao, C., Liu, F., 2020. Variation of soil carbon accumulation across a topographic gradient in a humid subtropical mountain forest. Biogeochemistry 149, 337–354. https://doi.org/10.1007/s10533-020-00679-2.

Turtureanu, P.D., Barros, C., Bec, S., Hurdu, B.-I., Saillard, A., Šibík, J., Balázs, Z.R., Novikov, A., Renaud, J., Podar, D., Thuiller, W., Pușcaș, M., Choler, P., 2020. Biogeography of intraspecific trait variability in matgrass (Nardus stricta): High phenotypic variation at the local scale exceeds large scale variability patterns. Perspect. Plant Ecol. Evol. Syst. 46, 125555. https://doi.org/10.1016/j.ppees.2020.125555.

Turtureanu, P.D., Pușcaș, M., Podar, D., Balázs, Z.R., Hurdu, B.-I., Novikov, A., Renaud, J., Saillard, A., Bec, S., Șuteu, D., Băcilă, I., Choler, P., 2023. Extent of intraspecific trait variability in ecologically central and marginal populations of a dominant alpine plant across European mountains. Ann. Bot. 132, 335–347. https://doi.org/10.1093/aob/mcad105.

Virto, I., Moni, C., Swanston, C., Chenu, C., 2010. Turnover of intra- and extra-aggregate organic matter at the silt-size scale. Geoderma 156, 1–10. https://doi.org/10.1016/j.geoderma.2009.12.028.

Voigt, C., Lamprecht, R.E., Marushchak, M.E., Lind, S.E., Novakovskiy, A., Aurela, M., Martikainen, P.J., Biasi, C., 2017. Warming of subarctic tundra increases emissions of all three important greenhouse gases – carbon dioxide, methane, and nitrous oxide. Glob. Chang. Biol. 23, 3121–3138. https://doi.org/10.1111/gcb.13563.

Von Lützow, M., Kögel-Knabner, I., Ekschmitt, K., Flessa, H., Guggenberger, G., Matzner, E., Marschner, B., 2007. SOM fractionation methods: Relevance to functional pools and to stabilization mechanisms. Soil Biol. Biochem. 39, 2183–2207. https://doi.org/10.1016/j.soilbio.2007.03.007.

Whitham, T.G., Bailey, J.K., Schweitzer, J.A., Shuster, S.M., Bangert, R.K., LeRoy, C.J., Lonsdorf, E.V., Allan, G.J., DiFazio, S.P., Potts, B.M., Fischer, D.G., Gehring, C.A., Lindroth, R.L., Marks, J.C., Hart, S.C., Wimp, G.M., Wooley, S.C., 2006. A framework for community and ecosystem genetics: from genes to ecosystems. Nat Rev Genet 7, 510–523. https://doi.org/10.1038/nrg1877.

Xia, Y., Yang, Y., 2019. RMSEA, CFI, and TLI in structural equation modeling with ordered categorical data: The story they tell depends on the estimation methods. Behav Res 51, 409–428. https://doi.org/10.3758/s13428-018-1055-2.

Zhang, T., 2005. Influence of the seasonal snow cover on the ground thermal regime: An overview. Rev. Geophys. 43. https://doi.org/10.1029/2004RG000157.

Zhu, M., Feng, Q., Qin, Y., Cao, J., Zhang, M., Liu, W., Deo, R.C., Zhang, C., Li, R., Li, B., 2019a. The role of topography in shaping the spatial patterns of soil organic carbon. Catena 176, 296–305. https://doi.org/10.1016/j.catena.2019.01.029.

Zhu, M., Mengxu, Z., Liu, W., Yanyan, Q., Deo, R., Zhang, C., 2019b. Effects of topography on soil organic carbon stocks in grasslands of a semiarid alpine region, northwestern China. J. Soil. Sediment. 19. https://doi.org/10.1007/s11368-018-2203-0.

Zhu, H., Wu, J., Guo, S., Huang, D., Zhu, Q., Ge, T., Lei, T., 2014. Land use and topographic position control soil organic C and N accumulation in eroded hilly watershed of the Loess Plateau. Catena 120, 64–72. https://doi.org/10.1016/j.catena.2014.04.007.